Spin dependent structure functions of the nucleon

F. Bissey,* Fu-Guang Cao,† and A. I. Signal‡

Institute of Fundamental Sciences PN461, Massey University, Private Bag 11 222, Palmerston North, New Zealand

(Received 29 December 2005; revised manuscript received 23 March 2006; published 15 May 2006)

We calculate the spin dependent structure functions $g_1(x)$ and $g_2(x)$ of the proton and neutron. Our calculation uses the meson cloud model of nucleon structure, which has previously given a good description of the HERMES data on polarized sea quark distributions, and includes all the leading contributions to spin dependent effects in this model. We find good agreement between our calculations and the current experimental data for the structure functions. We include in our calculations kinematic terms, which mix transverse and longitudinal spin components, for hadrons of spin $1/2$, 1, and $3/2$, and which can give considerable contributions to the g_2 structure functions. We also consider the possible interference terms between baryons or mesons in different final states with the same quantum numbers, and show that most of these terms do not give leading contributions to the spin dependent structure functions.

DOI: 10.1103/PhysRevD.73.094008 PACS numbers: 14.20.Dh, 11.30.Hv, 12.39.Ba, 13.88.+e

I. INTRODUCTION

The spin dependent structure functions of the nucleon are the subject of much theoretical and experimental interest. The main reason for this interest has been the large amount of evidence, starting with the EMC experiment [1] which strongly suggests that constituent quark models cannot fully describe the spin structure of protons and neutrons. This has led to considerable activity in order to determine how the spin of nucleons is built up from the intrinsic spin and orbital angular momentum of their constituent quarks and gluons.

Since 1988 further polarized deep inelastic scattering experiments have generally confirmed the EMC results for the proton-photon asymmetry A_1 and proton spin structure function $g_1(x)$ [2–4]. These measurements have also been performed on deuteron and neutron targets [5,6], which has enabled the Bjorken sum rule [7] to be tested at the five percent level.

In addition, there have been measurements, using transversely polarized targets, of the second nucleon-photon asymmetries A_2^N and the related structure functions $g_2^N(x)$ [8–12]. The $g_2(x)$ structure functions are of interest because they do not have a simple interpretation in the quark-parton model, but are related to transverse momentum of quarks and higher twist operators which measure correlations between quarks and gluons. The identification of a higher twist component in a measurement of $g_2^N(x)$ would be significant as this would give new information on the gluon field inside the nucleon, and its relationship with the quark fields.

Recently new experimental approaches have sought to augment the information available from deep inelastic scattering (DIS) experiments. These include semi-inclusive polarized DIS (HERMES and COMPASS), polarized proton-proton collisions (RHIC), and polarized photoproduction.

There have been a number of theoretical approaches to calculating $g_1(x)$ and $g_2(x)$ using phenomenological models of nucleon structure such as the MIT bag model [13–15] and the chiral soliton model [16–18]. In addition, there have been lattice calculations of some of the nucleon matrix elements of operators corresponding to small moments of the structure functions [19].

In this paper, we shall use the meson cloud model (MCM) to calculate the spin dependent structure functions of the nucleon. This model has been applied successfully in spin independent DIS, giving a good description of the HERA data on semi-inclusive DIS with a leading neutron [20,21], and also dijet events with a leading neutron [22,23]. In addition, the MCM gives a good description of the observed violation [24,25] of the Gottfried sum rule [26–28].

The MCM has been used previously to calculate $g_1(x)$ [29,30]. In those calculations pseudoscalar mesons were identified as the main constituents of the meson cloud. While these mesons do not directly contribute to the structure function, the presence of the cloud transfers some angular momentum from the quarks in the "bare" proton to the meson cloud and results in a decrease in the calculated first moment of g_1^p compared to the MIT bag model. More recently it has been realized that vector mesons, particularly the ρ, can also play a role in the spin structure of the proton [31]. In particular, these will give rise to flavor symmetry breaking in the sea, and the $\Delta\bar{u}(x) - \Delta\bar{d}(x)$ difference has been calculated by a number of authors [32,33]. Interestingly, these calculations predict that the spin dependent symmetry breaking is quite small, in contrast to the spin independent symmetry breaking combination $\bar{u}(x) - \bar{d}(x)$ which is observed to be large. Recently, these calculations were extended to the spin dependent sea distributions ($\Delta\bar{u}$, $\Delta\bar{d}$, Δs, $\Delta\bar{s}$) [34], and

*Electronic address: f.r.bissey@massey.ac.nz
†Electronic address: f.g.cao@massey.ac.nz
‡Electronic address: a.i.signal@massey.ac.nz

were found to be in good agreement with the recent results from HERMES [35].

In this paper we revisit the earlier calculations of $g_1^N(x)$ in light of the developments in the MCM since that time. We also extend the calculations of structure functions using the MCM to $g_2^N(x)$, and investigate the kinematic regions where it may be possible to observe a twist-3 piece of the structure functions.

In Sec. II of this paper we present the formalism for discussing spin dependent structure functions in the meson cloud model, including a discussion of the kinematic terms which lead to g_1 of cloud components contributing to g_2 of the nucleon (and vice versa) [33]. Contributions to the structure functions from interference between different states of the cloud [32] are discussed in Sec. III, and it is shown that most of the leading interference contributions vanish. In Sec. IV we apply the MCM formalism and determine all the necessary momentum distributions of the components of the meson cloud. We also discuss the correct prescription to use in describing the energy of the intermediate state hadrons in the MCM. In Sec. V we calculate the spin dependent structure functions of the baryons and mesons in the cloud using the MIT bag model. The numerical results for the nucleon structure functions are shown and discussed in Sec. VI. In the last section we summarize our findings.

II. SPIN DEPENDENT STRUCTURE FUNCTIONS IN THE MESON CLOUD MODEL

In the LAB frame the cross section for inclusive inelastic lepton-nucleon scattering may be written in terms of the product of lepton and hadron tensors

$$\frac{d^2\sigma}{d\Omega dE'} = \frac{\alpha^2}{q^4}\frac{E'}{E}L_{\mu\nu}W^{\mu\nu}, \tag{1}$$

where α is the fine structure constant, $E(E')$ is the energy of the incident (scattered) lepton, and q^2 is the squared four-momentum transfer. In spin dependent (polarized) scattering we are interested in the antisymmetric part of the hadron tensor $W^A_{\mu\nu}$, which can be written in terms of two structure functions G_1 and G_2 [36]

$$W^A_{\mu\nu} = \frac{i}{m_N}\epsilon_{\mu\nu\rho\sigma}q^\rho\Big[s_N^\sigma G_1(\nu, Q^2) + \frac{s_N^\sigma p_N\cdot q - p_N^\sigma s_N\cdot q}{m_N^2}G_2(\nu, Q^2)\Big]. \tag{2}$$

Here ν is the energy transfer, $Q^2 = -q^2$, and s_N^μ is the nucleon spin vector, normalized to $s_N^2 = -m_N^2$. In the Bjorken limit ($Q^2, \nu \to \infty$) the structure functions scale, modulo perturbative QCD logarithmic evolution in Q^2,

$$\frac{\nu}{m_N}G_1(\nu, Q^2) \to g_1(x) \qquad \frac{\nu^2}{m_N^2}G_2(\nu, Q^2) \to g_2(x), \tag{3}$$

where the scaling variable $x = Q^2/(2m_N\nu)$ lies between 0 and 1. In this limit we have

$$W^A_{\mu\nu} = i\epsilon_{\mu\nu\rho\sigma}q^\rho\Big[\frac{s_N^\sigma}{p_N\cdot q}g_1(x) + \frac{s_N^\sigma p_N\cdot q - p_N^\sigma s_N\cdot q}{(p_N\cdot q)^2}g_2(x)\Big]. \tag{4}$$

In order to discuss the structure functions separately we use a projection operator

$$P_{\mu\nu} = \frac{i}{2p_N\cdot q}\epsilon_{\mu\nu\alpha\beta}q^\alpha s_N^\beta, \tag{5}$$

such that

$$P^{\mu\nu}W^A_{\mu\nu}(p_N, s_N, q) = \frac{m_N^2q^2 + (s_N\cdot q)^2}{(p_N\cdot q)^2}g_1(x) - \gamma^2 g_2(x), \tag{6}$$

where

$$\gamma^2 = \frac{4x^2m_N^2}{Q^2}. \tag{7}$$

In the MCM [37,38], the nucleon can be viewed as a bare nucleon plus some baryon-meson Fock states which result from the fluctuation of nucleon to baryon plus meson $N \to MB$. The wave function of the nucleon can be written as [29]

$$|N\rangle_{\text{physical}} = \sqrt{Z}|N\rangle_{\text{bare}} + \sum_{MB}\sum_{\lambda_M\lambda_B}\int dyd^2\mathbf{k}_\perp\phi_{MB}^{\lambda_M\lambda_B}(y, k_\perp^2) \times |M^{\lambda_M}(y, \mathbf{k}_\perp); B^{\lambda_B}(1-y, -\mathbf{k}_\perp)\rangle. \tag{8}$$

Here Z is the wave function renormalization constant and $\phi_{MB}^{\lambda_M\lambda_B}(y, k_\perp^2)$ is the wave function of the Fock state containing a meson (M) with longitudinal momentum fraction y, transverse momentum $\mathbf{k}_\perp$, and helicity λ_M, and a baryon (B) with momentum fraction $1-y$, transverse momentum $-\mathbf{k}_\perp$, and helicity λ_B. The model assumes that the lifetime of a virtual baryon-meson Fock state is much longer than the interaction time in the deep inelastic or Drell-Yan process, thus scattering from the virtual baryon-meson Fock states can contribute to the observed structure functions of the nucleon, as shown in Fig. 1.

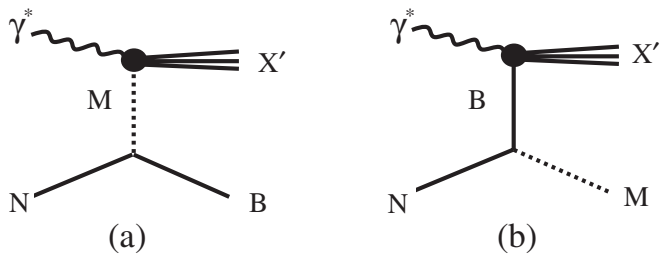

FIG. 1. The photon may be scattered from (a) virtual meson and (b) virtual baryon.

The contribution to the nucleon tensor $W_{\mu\nu}$ from processes such as that in Fig. 1, where the virtual photon interacts with a component of the cloud (such as a ρ meson), is given by

$$\delta W_{\mu\nu} = \int \frac{d^3p_B}{(2\pi)^3}\frac{m_M}{m_B}\sum_{\lambda,\lambda'}|J_{NMB}|^2 W^M_{\mu\nu}(k, s_M, q), \quad (9)$$

where s_M is the meson spin vector (normalized to $s_M^2 = -m_M^2$), and $J_{NMB}(p_N, k, p_B, s_N, s_M, s_B)$ is the meson propagator multiplied by the NMB vertex. The meson tensor here is defined by

$$W^M_{\mu\nu}(k, s_M, q) = \frac{1}{2\pi}\sum_X (2\pi)^4\delta^4(k + q - p_X)\langle k, s_M|J_\mu|X\rangle \times \langle X|J_\nu|k, s_M\rangle. \quad (10)$$

As first shown by Sullivan [37], the meson contribution to the nucleon tensor is expressed in terms of the meson tensor and the nucleon-meson-baryon vertex, and this leads to the contribution being expressed as a convolution between the meson tensor and the probability distribution for finding the meson in the cloud with momentum fraction y, e.g.

$$\delta F_2^N(x) = \int_x^1 dy f_{\rho N/N}(y)F_2^\rho\left(\frac{x}{y}\right) \quad (11)$$

gives the contribution to the nucleon structure function F_2 arising from the virtual photon interacting with the ρ meson from the $N \to N\rho$ part of the meson cloud.

Baryon or meson components of the cloud with spin $\geq 1/2$ will contribute directly to the antisymmetric part of the nucleon tensor. We consider three cases of interest.

A. Spin 1/2 baryons

A spin $1/2$ baryon in the cloud, such as a nucleon or a Λ, has the antisymmetric part of its tensor similar to Eq. (4), with the nucleon mass, momentum, and spin vector replaced by m_B, k (the baryon four momentum), and s_B, respectively. Multiplying by the projection operator $\tilde{P}^{\mu\nu} = (m_N/m_B)P^{\mu\nu}$, where $P^{\mu\nu}$ is given in Eq. (5), gives

$$\tilde{P}^{\mu\nu}W^{(1/2)A}_{\mu\nu}(k, s_B, q) = \frac{m_N}{m_B}[A_1 g_1^B(k, q) + A_2 g_2^B(k, q)], \quad (12)$$

where we have the coefficients

$$A_1 = \frac{1}{p_N\cdot q k\cdot q}(s_N\cdot q s_B\cdot q - q^2 s_N\cdot s_B), \quad (13)$$

$$A_2 = \frac{q^2}{p_N\cdot q(k\cdot q)^2}(s_N\cdot k s_B\cdot q - k\cdot q s_N\cdot s_B) \quad (14)$$

and the structure functions g_i^B are those for the spin $1/2$ baryon. In what follows we will use time-ordered perturbation theory (TOPT), which has the advantage that all the baryon and meson structure functions that are required are those for on-shell hadrons. We can now write the contributions of the spin $1/2$ baryon to the observed nucleon structure functions as convolutions [33]

$$\frac{m_N^2q^2 + (s_N\cdot q)^2}{(p_N\cdot q)^2}\delta g_1(x) - \gamma^2\delta g_2(x) = \int_x^{y_{\max}}\frac{dy}{y}\left[B_1(y)g_1^B\left(\frac{x}{y}, Q^2\right) + B_2(y)g_2^B\left(\frac{x}{y}, Q^2\right)\right], \quad (15)$$

where $y_{\max}$ is the maximum allowable value of the momentum fraction $y = k\cdot q/p_N\cdot q$, which is usually 1, and the baryon momentum distributions are

$$B_{1,2}(y) = \int_0^{(k_\perp^2)_{\max}} d\vec{k}_\perp^2\int_0^{2\pi}d\phi\frac{|\vec{p}_N|}{(2\pi)^3}y\frac{\partial y'}{\partial y}\sum_{\lambda_B,\lambda_M}|J_{NBM}|^2A_{1,2}. \quad (16)$$

Here y' is the longitudinal momentum fraction

$$\vec{k} = \vec{k}_\perp + y'\vec{p}_N \quad (17)$$

which, in the infinite momentum frame ($|\vec{p}_N| \to \infty$), is related to y by

$$y' = \frac{y}{1+\sqrt{1+\gamma^2}}\left[1 + \sqrt{1 + \frac{\gamma^2}{y^2m_N^2}(\vec{k}_\perp^2 + m_B^2)}\right]. \quad (18)$$

Most previous calculations of structure functions in the MCM have not taken into account the difference between the light-cone momentum fraction y and the longitudinal momentum fraction y', as these are the same in the Bjorken limit. However, at finite Q^2 the difference is not negligible.

The maximum transverse momentum squared is

$$(k_\perp^2)_{\max} = \frac{m_N^2}{\gamma^2}(1+\sqrt{1+\gamma^2})(1-2y+\sqrt{1+\gamma^2}) - m_B^2 \to Q^2\frac{1-y}{x^2} - m_B^2 \gg m_N^2, \quad (19)$$

which at small x is much larger than any momentum cutoff that is required for the vertex, so $(k_\perp^2)_{\max}$ may safely be taken to infinity.

From Eq. (15) we see that the nucleon structure functions pick up contributions from both g_1^B and g_2^B of the baryon in the cloud. This occurs because the spin vector of the cloud baryon s_B^μ is not parallel to the initial nucleon spin vector s_N^μ. So if the initial nucleon is longitudinally polarized, the baryon in the cloud will have both longitudinal and transverse spin components, and hence g_2^B will give a finite contribution to g_1^N. Similarly g_2^N will get a contribution from g_1^B. As the bare g_2^N structure functions are expected to be small, this kinematic contribution from the baryon-meson cloud could be a major portion of these structure functions.

Following Ref. [33] we write Eq. (15) in terms of the nucleon and baryon helicities, λ_N and λ_B, and the nucleon transverse spin vector $s_N^\top$

$$\left(\lambda_N^2 - \frac{|s_N^\top|^2}{m_N^2}\gamma^2\right)\delta g_1(x) - \gamma^2 \delta g_2(x) = \sum_{\lambda_B}\lambda_B \int_x^{y_m} \frac{dy}{y}\left\{\left[\lambda_N^2 f_{1L}(y) + \frac{|s_N^\top|^2}{m_N^2} f_{1T}(y)\right] g_1^B\left(\frac{x}{y}, Q^2\right) + \left[\lambda_N^2 f_{2L}(y) + \frac{|s_N^\top|^2}{m_N^2} f_{2T}(y)\right] g_2^B\left(\frac{x}{y}, Q^2\right)\right\}, \tag{20}$$

where the momentum distributions $f_{1,2L,T}(y)$ are similar (up to signs) to those given in Eqs. (2.25–2.28) of Ref. [33] with m_V and λ_V replaced by m_B and λ_B, respectively. We give these expressions in Appendix A below.

By combining the longitudinal $\lambda_N = 1(|s_N^\top|/m_N \equiv \tau_N = 0)$ with the transverse $\lambda_N = 0(\tau_N = 1)$ amplitude in Eq. (20), and defining the functions

$$\Delta f^1_{1,2L,T}(y) = f^{\lambda=+1}_{1,2L,T}(y) - f^{\lambda=-1}_{1,2L,T}(y), \tag{21}$$

we can obtain the separate contributions to the nucleon g_1 and g_2 structure functions:

$$\delta g_1(x, Q^2) = \frac{1}{1+\gamma^2}\int_x^1 \frac{dy}{y}\sum_{i=1,2}[\Delta f^1_{iL}(y) - \Delta f^1_{iT}(y)] g_i^B\left(\frac{x}{y}, Q^2\right) \tag{22}$$

$$\delta g_2(x, Q^2) = -\frac{1}{1+\gamma^2}\int_x^1 \frac{dy}{y}\sum_{i=1,2}\left[\Delta f^1_{iL}(y) + \frac{\Delta f^1_{iT}(y)}{\gamma^2}\right] g_i^B\left(\frac{x}{y}, Q^2\right). \tag{23}$$

B. Spin 1 mesons

The analysis for spin 1 mesons exactly follows that above for spin $1/2$ baryons, and was given by Kumano and Miyama [33]. The reason for this is that the most general form of the antisymmetric part of the meson tensor is the same for spin 1 mesons as for spin $1/2$ baryons [39]. Hence, the results of the previous subsection can be directly translated to the vector meson case, simply by replacing m_B and λ_B by m_M and λ_M, respectively, and replacing the baryon structure functions by meson structure functions.

Interestingly, the symmetric part of the meson tensor for spin 1 mesons contains two additional terms, which are both proportional to the structure function $b_1^M(x)$ at leading twist (via a generalized Callan-Gross relation). This would lead to a contribution to the nucleon structure function $F_2(x)$ coming from (for example) b_1^ρ, though it is expected that this will be rather small compared to the dominant MCM contribution coming from the pions in the cloud via F_2^π.

C. Spin 3/2 baryons

The number of independent Lorentz invariant structure functions for a spin J hadron increases approximately linearly with J. If $A^J_{hH,h'H'}$ are the imaginary part of the forward Compton helicity amplitudes for $\gamma_h + \text{hadron}^J_H \to \gamma_{h'} + \text{hadron}^J_{H'}$, it can be seen that there are $6J + 2$ $(6J + 1)$ independent amplitudes for J-integer (half-integer) satisfying P and T invariance and helicity conservation. Of these, $2J$ $(2J + 1)$ amplitudes contribute to spin dependent scattering. Thus, the general expression for the antisymmetric part of the hadronic tensor for a particle of spin J is [39]

$$W^A_{\mu\nu} = \sum_{L=1,3\ldots}^{2J} i\frac{{}^J_L g_1}{\nu^L}\epsilon^{\mu\nu\alpha\mu_1}\theta_{\mu_1\mu_2\ldots\mu_L} q_\alpha q^{\mu_2}\cdots q^{\mu_L} + \sum_{L=1,3\ldots}^{2J} i\frac{{}^J_L g_2}{\nu^{L+1}}\epsilon^{\mu\nu\alpha\beta} p_{[\mu_1}\theta_{\beta]\mu_2\ldots\mu_L} q_\alpha q^{\mu_1}\cdots q^{\mu_L}. \tag{24}$$

In this expression $\theta^{\mu_1\mu_2\ldots\mu_L}$ is a completely symmetric, traceless pseudotensor. It can be thought of as a generalized Pauli-Lubanski spin vector. For spin $1/2$ and spin 1 only θ^μ is nonvanishing, and it is proportional to the usual spin vector s^μ. The structure functions ${}^J_L g_{1,2}$ are generalizations of the usual spin dependent structure functions. At leading twist we have

$${}^J_L g_1 = \sum_{H=-J}^{J}\langle J, H, J, -H|L, 0\rangle q^{JH}_\uparrow \qquad {}^J_L g_2 = 0, \tag{25}$$

and for $J = 3/2$ in particular

$$\begin{aligned} {}^{3/2}_1 g_1 &= \frac{1}{\sqrt{20}}(3q^{(3/2)(3/2)}_\uparrow - 3q^{(3/2)(3/2)}_\downarrow + q^{(3/2)(1/2)}_\uparrow - q^{(3/2)(1/2)}_\downarrow) \\ {}^{3/2}_3 g_1 &= \frac{1}{\sqrt{20}}(q^{(3/2)(3/2)}_\uparrow - q^{(3/2)(3/2)}_\downarrow - 3q^{(3/2)(1/2)}_\uparrow + 3q^{(3/2)(1/2)}_\downarrow). \end{aligned} \tag{26}$$

The polarization vectors for a spin $3/2$ particle have a spinor nature [40] which slightly complicates the expression for the Pauli-Lubanski vector

$$s^\mu\left(\tfrac{3}{2}, \lambda\right) = \tfrac{3}{2} i\epsilon^{\mu\rho\sigma\tau}\,\mathrm{Tr}[\bar{E}_\rho(\lambda)E_\sigma(\lambda)]p_\tau, \tag{27}$$

where λ can take the values $\pm 1/2$, $\pm 3/2$, and the trace is taken over spinor indices. We have the normalization $s^2 = -\lambda^2 M^2$.

As in the spin $1/2$ and spin 1 cases, we can take $\theta^\mu \propto s^\mu$. We also require $\theta^{\mu\nu\rho}$ in the spin $3/2$ case. We take the

traceless combination of symmetric pseudotensors

$$\theta^{\mu\nu\rho} \propto \frac{1}{\lambda^2} s^\mu s^\nu s^\rho + \mathcal{S}(s^\mu p^\nu p^\rho), \tag{28}$$

where $\mathcal{S}$ symmetrizes over the Lorentz indices. After some work we obtain

$$W^A_{\mu\nu} = i\epsilon_{\mu\nu\rho\sigma}q^\rho\Big[\frac{s^\sigma}{\nu}\Big(\frac{2}{\sqrt{5}}\,{}^{3/2}_{1}g_1 - \frac{2\omega^2}{2\sqrt{5}}\,{}^{3/2}_{3}g_1\Big) - \frac{4}{3\sqrt{5}}\frac{p^\sigma s\cdot q}{\nu^2}\,{}^{3/2}_{3}g_1 + \Big(\frac{s^\sigma}{\nu} - \frac{p^\sigma s\cdot q}{\nu^2}\Big) \times \Big(\frac{2}{\sqrt{5}}\,{}^{3/2}_{1}g_2 - \frac{2\omega^2}{2\sqrt{5}}\,{}^{3/2}_{3}g_1\Big)\Big], \tag{29}$$

where

$$\omega^2 = 1 + \frac{(s\cdot q)^2}{\lambda^2\nu^2} \tag{30}$$

which goes to 2 in the Bjorken limit.

We can now follow the same steps as for spin $1/2$ and spin 1 hadrons to obtain the MCM contributions to the spin dependent structure functions of the nucleon. In this case the generalizations of the coefficients A_i and B_i above depend on the helicity of the struck baryon, so it is useful to rewrite the spin $3/2$ structure functions as g_i^{JH} which depend only on one helicity state. We have

$$\begin{aligned} g_i^{(3/2)(3/2)} &= \frac{3}{2\sqrt{5}}\,{}^{3/2}_{1}g_i + \frac{1}{2\sqrt{5}}\,{}^{3/2}_{3}g_i \\ g_i^{(3/2)(1/2)} &= \frac{1}{2\sqrt{5}}\,{}^{3/2}_{1}g_i - \frac{3}{2\sqrt{5}}\,{}^{3/2}_{3}g_i. \end{aligned} \tag{31}$$

This gives

$$\begin{aligned} \tilde{P}^{\mu\nu}W^{(3/2)A}_{\mu\nu}(k, s_B, \lambda, q) = \frac{m_N}{m_B}[&A_1^{3/2}g_1^{(3/2)(3/2)}(k,q) \\ &+ A_1^{1/2}g_1^{(3/2)(1/2)}(k,q) \\ &+ A_2^{3/2}g_2^{(3/2)(3/2)}(k,q) \\ &+ A_2^{1/2}g_2^{(3/2)(1/2)}(k,q)], \end{aligned} \tag{32}$$

where the coefficients are linear combinations of A_1 and A_2 from Eq. (14)

$$\begin{aligned} A_1^{3/2} &= \frac{14-2\omega^2}{15}A_1 + \frac{4}{15}A_2 \qquad A_1^{1/2} = \frac{6+2\omega^2}{5}A_1 - \frac{4}{5}A_2 \\ A_2^{3/2} &= \frac{18-2\omega^2}{15}A_2 \qquad A_2^{1/2} = \frac{2+2\omega^2}{15}A_2 \end{aligned} \tag{33}$$

and

$$\omega^2 = 1 + \Big[1 - \frac{m_H^2}{yy'm_N^2}(1-\sqrt{1+\gamma^2})\Big]^2. \tag{34}$$

Now doing the required integrations (details can be found in Appendix A), we end up with a result similar to Eq. (23):

$$\delta g_1(x,Q^2) = \frac{1}{1+\gamma^2}\int_x^1\frac{dy}{y}\sum_{i=1,2}\sum_{h=1/2,3/2}[\Delta f_{iL}^{(3/2)h}(y) - \Delta f_{iT}^{(3/2)h}(y)]g_i^{3/2h}\Big(\frac{x}{y},Q^2\Big) \tag{35}$$

$$\delta g_2(x,Q^2) = -\frac{1}{1+\gamma^2}\int_x^1\frac{dy}{y}\sum_{i=1,2}\sum_{h=1/2,3/2}\Big[\Delta f_{iL}^{(3/2)h}(y) + \frac{\Delta f_{iT}^{(3/2)h}(y)}{\gamma^2}\Big]g_i^{(3/2)h}\Big(\frac{x}{y},Q^2\Big). \tag{36}$$

III. INTERFERENCE CONTRIBUTIONS

In polarized DIS, we can consider the possibility of interference terms between intermediate states containing different hadrons. This possibility is allowed in polarized DIS as the observed spin dependent structure functions do not contribute to the total γ^*N cross section, but only to $\Delta\sigma = \sigma_{3/2} - \sigma_{1/2}$ or, equivalently, to σ_I the cross section associated with interference between transverse and longitudinal polarizations of the virtual photon [36]. Previous authors have considered interference between π and ρ mesons [32,41], π and σ mesons [42], K and K^* mesons [43], and N and Δ baryons [30,34,44]. We show an example of an interference term in Fig. 2.

The interference terms between mesons of different helicity are particularly interesting as they appear to offer a mechanism whereby angular momentum in the cloud can be directly coupled to quarks, possibly giving rise to large sea quark polarizations [41]. However, care needs to be taken over which interference terms can actually contribute to the observed structure functions. Let $\tilde{A}_{hH,h'H^*}$ be the imaginary part of the forward helicity amplitude for the interference term $\gamma_h + \text{hadron1}_H \to \gamma_{h'} + \text{hadron2}_{H^*}$. In the Bjorken limit quark helicity is conserved, which implies that the only amplitudes that contribute to $\Delta\sigma$ are in the combinations $(\tilde{A}_{1H,1H^*=H} - \tilde{A}_{-1H,-1H^*=H})$. Also the generalization of the Callen-Gross relation gives $\tilde{A}_{0H,0H^*=H} \to 0$. These two results imply that for (pseudo)-scalar mesons interfering with (pseudo)vector mesons only combinations of amplitudes $(\tilde{A}_{10,10^*} - \tilde{A}_{-10,-10^*})$ can contribute to the structure function. However, this combination

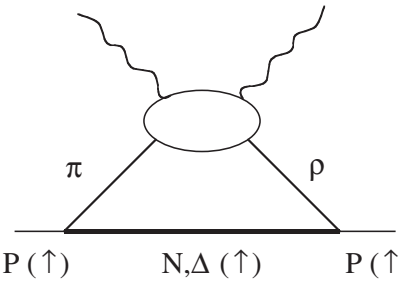

FIG. 2. Interference between π and ρ mesons.

will be zero by parity invariance, meaning that interference between mesons cannot contribute to the leading twist structure functions. Amplitudes like $\tilde{A}_{10,0H^*=1}$ can contribute to the interference cross section σ_I between transverse and longitudinal photon polarizations at higher twist.

In the case of interference between N and Δ baryons, this contribution involves the combination of amplitudes $(\tilde{A}_{1(1/2),1H^*=1/2} - \tilde{A}_{-1(1/2),-1H^*=1/2})$ which need not vanish.

We can write the contribution of interference terms to the nucleon tensor $W_{\mu\nu}$, where the two particles that interfere are labeled X and Y and the spectator hadron is labeled by S:

$$\delta W^{XY}_{\mu\nu}(p_N, s_N, q) = \int \frac{d^3p_s}{(2\pi)^3} \frac{2\sqrt{m_X m_Y} m_S}{E_S} \times \sum_{\lambda_X,\lambda_Y,\lambda_S} [J_{NXS} J^*_{NYS} W^{X\to Y}_{\mu\nu}(k_X, s_X, k_Y, s_Y, q) + J_{NXS} J^*_{NYS} W^{Y\to X}_{\mu\nu}(k_Y, s_Y, k_X, s_X, q)], \tag{37}$$

where the interference tensor is given by

$$W^{X\to Y}_{\mu\nu}(k_X, s_X, k_Y, s_Y, q) = \frac{1}{4\pi\sqrt{m_X m_Y}} \sum_{X',Y'} \delta^4(p^2_{X'} - m^2_{X'}) \times \delta^4(p^2_{Y'} - m^2_{Y'}) \langle k_X, s_X | J_\mu | X' \rangle \times \langle Y' | J^\dagger_\nu | k_Y, s_Y \rangle. \tag{38}$$

We see that the interference tensors in Eq. (37) are related by

$$W^{Y\to X}_{\mu\nu}(k_Y, s_Y, k_X, s_X, q) = [W^{X\to Y}_{\nu\mu}(k_X, s_X, k_Y, s_Y, q)]^*. \tag{39}$$

This enables us to write the contribution to the nucleon tensor as

$$\delta W^{XY}_{\mu\nu}(p_N, s_N, q) = \int \frac{d^3p_s}{(2\pi)^3} \frac{2\sqrt{m_X m_Y} m_S}{E_S} \times \sum_{\lambda_X,\lambda_Y,\lambda_S} 2\mathcal{R}[J_{NXS} J^*_{NYS}] \times W^{X\to Y}_{\mu\nu}(k_X, s_X, k_Y, s_Y, q). \tag{40}$$

In TOPT, the 3-vectors of the interfering particles $\vec{k}_{X,Y}$ will be identical, however their energies are not, as both particles are on-shell. We introduce two momentum fractions

$$y_{X,Y} = \frac{k_{X,Y} \cdot q}{p_N \cdot q}, \tag{41}$$

noting that the longitudinal momentum fraction y' is the same for both hadrons. If we define

$$k^\mu = \tfrac{1}{2}(k^\mu_X + k^\mu_Y), \qquad \delta k^\mu = \tfrac{1}{2}(k^\mu_X - k^\mu_Y) \tag{42}$$

$$y = \tfrac{1}{2}(y_X + y_Y), \qquad \delta y = \tfrac{1}{2}(y_X - y_Y) \tag{43}$$

$$s^\mu = \tfrac{1}{2}(s^\mu_X + s^\mu_Y), \qquad \delta s^\mu = \tfrac{1}{2}(s^\mu_X - s^\mu_Y), \tag{44}$$

then in the Bjorken limit we have $\delta k \to 0$, $\delta y \to 0$, and $\delta s \to 0$.

We can now write the most general form of the antisymmetric tensor for the interference term

$$\delta W^{(A)XY}_{\mu\nu} = i\epsilon_{\mu\nu\rho\sigma} q^\rho \Big[\frac{s^\sigma}{k\cdot q} g^{XY}_1 + \Big(\frac{s^\sigma}{k\cdot q} - \frac{s\cdot q}{(k\cdot q)^2} k^\sigma \Big) g^{XY}_2 + \frac{\delta s^\sigma}{k\cdot q} \tilde{g}^{XY}_1 + \frac{s\cdot q}{(k\cdot q)^2} \delta k^\sigma \tilde{g}^{XY}_2 \Big] + i \frac{\tilde{k}^\mu_X \tilde{k}^\nu_Y - \tilde{k}^\nu_X \tilde{k}^\mu_Y}{2k\cdot q} \tilde{a}^{XY}_1 + i \frac{\tilde{s}^\mu_X \tilde{s}^\nu_Y - \tilde{s}^\nu_X \tilde{s}^\mu_Y}{2k\cdot q} \tilde{a}^{XY}_2, \tag{45}$$

where we denote $\tilde{v}^\mu = (v^\mu - u\cdot q q^\mu/q^2)$ for any four vector v. This includes four possible new interference "structure functions." All of these new terms arise from our use of TOPT, and would vanish in a covariant formulation. However, the price to be paid in the covariant formulation is that we would have to use structure functions of off-shell hadrons, which are difficult to define and measure. As $\delta k \approx [(m^2_Y - m^2_X)/(4y'p), \vec{0}]$ and $\delta s \approx \lambda\{0, [(m^2_Y - m^2_X)/(4(y'p)^2)]\vec{k}_\perp, (m^2_Y - m^2_X)/(4y'p)\}$, the contributions from $\tilde{g}^{XY}_{1,2}$ will be kinematically suppressed, and look like higher twist corrections to the observed g_1 and g_2.

The two structure functions $\tilde{a}^{XY}_1$ and $\tilde{a}^{XY}_2$ involve antisymmetric combinations of hadron four vectors and are independent of polarization. These terms do not give any contribution to the nucleon structure functions because when the projector $\tilde{P}^{\mu\nu}$ is applied to them we obtain a coefficient A^{XY}_i which is proportional to $\sin\phi$. Integration over ϕ then results in these terms being zero. This agrees with our earlier observation that interference involving (pseudo) scalar mesons and (pseudo) vector or scalar mesons does not contribute at leading twist, as this violates parity invariance.

In a similar fashion to our procedure in the previous section, we multiply the antisymmetric interference tensor by the projector $\tilde{P}^{\mu\nu} = (m_N/\sqrt{m_X m_Y}) P^{\mu\nu}$, which gives

$$\tilde{P}^{\mu\nu} \delta W^{(A)XY}_{\mu\nu} = \frac{m_N}{\sqrt{m_X m_Y}} [A^{XY}_1 g^{XY}_1 + \tilde{A}^{XY}_1 \tilde{g}^{XY}_1 + A^{XY}_2 g^{XY}_2 + \tilde{A}^{XY}_2 \tilde{g}^{XY}_2], \tag{46}$$

where

$$A^{XY}_1 = \frac{1}{p_N\cdot q k\cdot q} (s_N\cdot q s\cdot q - q^2 s_N\cdot s) \tag{47}$$

$$\tilde{A}^{XY}_1 = \frac{1}{p_N\cdot q k\cdot q} (s_N\cdot q \delta s\cdot q - q^2 s_N\cdot \delta s) \tag{48}$$

$$A_2^{XY} = \frac{q^2}{p_N \cdot q(k \cdot q)^2}(s_N \cdot k s \cdot q - k \cdot q s_N \cdot s) \quad (49)$$

$$\tilde{A}_2^{XY} = \frac{s \cdot q}{p_N \cdot q(k \cdot q)^2}(s_N \cdot q \delta k \cdot q - q^2 s_N \cdot \delta k). \quad (50)$$

We observe that A_1^{XY} and A_2^{XY} are the same (up to mass factors) as the coefficients given in Eqs. (13) and (14) for spin $1/2$ baryons in the cloud. For the other two coefficients, we find

$$\tilde{A}_1^{XY} = \lambda\lambda_N \frac{m_X^2 - m_Y^2}{4yy' m_N^2}(1 - \sqrt{1+\gamma^2}) \quad (51)$$

$$\tilde{A}_2^{XY} = -\tilde{A}_1^{XY}\left(1 - \frac{m_X^2 - m_Y^2}{yy' m_N^2}(1 - \sqrt{1+\gamma^2})\right), \quad (52)$$

which both vanish in the Bjorken limit.

In the expression for the interference tensor [Eq. (40)] we can write the part of the integrand that depends on the vertices as a sum of polarization independent plus longitudinal and transverse terms

$$\frac{2\sqrt{m_X m_Y} m_S}{(2\pi)^3 E_S} \sum_{\lambda_S} 2\mathcal{R}[J_{NXS} J_{NYS}^*] = C_0^\lambda(\phi) + \lambda_N C_L^\lambda(\phi) + \tau_N C_T^\lambda(\phi), \quad (53)$$

where ϕ is the angle between $k_\perp$ and $\vec{s}_N^{\,\top}$, $\tau_N = |\vec{s}_N^{\,\top}|/m_N$ and λ labels the helicity of the struck hadron. If we consider the case of interference between a pion and a rho with helicity ± 1, we find that C_0 is zero while C_L and C_T are not. When combined with the appropriate A_i^{XY} coefficients and integrated over ϕ, we find that these contributions are zero. Hence, there are no contributions to the interference tensor from interference between π and ρ mesons. Similar conclusions can also be drawn about any contributions from interference between K and K^* mesons. Interference between N and Δ baryons also appears to be suppressed. We find that when the spectator meson is a pion the coefficients C_0, C_L, and C_T are nonzero, however their angular dependence is proportional to terms like $\cos\phi$, $\sin\phi$, or $\cos 2\phi$, all of which again integrate to zero when combined with the appropriate coefficients. Details of this calculation are in Appendix B below. In the case of the spectator meson being a ρ meson the coefficients are very difficult to calculate because of the complicated gamma structure of the two vertices. However, this contribution is already greatly suppressed because of the small probability of the $|\Delta\rho\rangle$ state. Thus interference contributions to the polarized structure functions are mostly zero or very small in the meson cloud model, and we shall henceforth neglect them.

Our conclusions regarding the contributions of interference terms are different from those of earlier authors who considered these terms [30,32,34,41–44]. These earlier works generally calculated interference terms by considering separately J_{NXS} and J_{NYS} as given in Appendix B of Ref. [29], or similar, which are worked out from considering the direct processes. However, it appears that these calculations of the vertex factors have not followed the same, or consistent, phase conventions when considering different vertices. This is not important when considering direct processes, as all terms are proportional to $|J|^2$, but for interference terms involving $J_{NXS} J_{NYS}^*$, any change in relative phase between the two vertices renders the calculation meaningless. In this work we have not calculated the two vertices separately, but considered the complete interference process. The advantage of this is that the two amplitudes for the processes $XS \to YS$ and $YS \to XS$ must be added. As these two amplitudes are conjugate, the result must be real, which gives a check that the phase factors have been correctly accounted for. More details are given in Appendix B.

IV. SPIN DEPENDENT MOMENTUM DISTRIBUTIONS OF MESONS AND BARYONS IN THE CLOUD

We now turn to the calculation of the various momentum distributions $\Delta f(y)$ of the components of the cloud. In general, these distributions are of the form (up to kinematic factors given in the previous section and Appendix A)

$$\Delta f_{BM} \sim \int_0^{(k_\perp^2)_m} dk_\perp^2 J_{NBM}^{\lambda_1\lambda_2}(y, k_\perp^2)(J_{NBM}^{\lambda_1\lambda_2}(y, k_\perp^2))^\dagger. \quad (54)$$

In this case J_{NBM} is the nucleon-baryon-meson vertex function multiplied by the propagator of the struck component of the cloud, i.e.

$$J_{NBM}^{\lambda_1\lambda_2} \propto \frac{V(\vec{p}, \uparrow; \vec{k}, \lambda_1, \vec{p}', \lambda_2)}{E_N - E_M - E_B}, \quad (55)$$

which is the amplitude that a nucleon with momentum $\vec{p}$ and helicity $+1/2$ is found in a meson cloud Fock state where the struck hadron has momentum $\vec{k}$ and helicity λ_1 and the spectator hadron has momentum $\vec{p}'$ and helicity λ_2. Note that we have explicitly used TOPT to write the propagator of the struck particle being proportional to the energy denominator in this expression.

In the infinite momentum frame (IMF), $p = |\vec{p}| \to \infty$, Drell, Levy, and Yan [45] (building on earlier work by Weinberg [46]) showed that contributions from Fock states containing antiparticles vanish and also that only the contributions with forward moving ($y \geq 0$) particles contribute. As we saw earlier, all relevant momenta can be expressed in terms of y, which we take as the longitudinal momentum proportion carried by the meson, and $\vec{k}_\perp$. The amplitude is now proportional to

$$\frac{V_{IMF}^{\lambda_1\lambda_2}(y, k_\perp^2)}{m_N^2 - M_{BM}^2(y, k_\perp^2)}, \quad (56)$$

where

$$M_{BM}^2(y,k_\perp^2)=\frac{m_M^2+k_\perp^2}{y}+\frac{m_B^2+k_\perp^2}{1-y} \tag{57}$$

is the invariant mass squared of the Fock state.

Using TOPT guarantees that, for a given $|BM\rangle$ component of the cloud, the probability of finding the meson M with longitudinal momentum fraction y is equal to that of finding the baryon B with longitudinal momentum fraction $1-y$. This is not necessarily true in a covariant approach [29], which leads to nonconservation of charge and momentum. However, a problem arises in TOPT when the vertex contains derivative coupling between fields [e.g. the usual pseudovector ρNN vertex contains a term proportional to $\bar{\psi}\sigma_{\mu\nu}(\partial^\mu\theta^\nu-\partial^\nu\theta^\mu)\psi$ where ψ is the nucleon field and θ is the vector field], as these terms introduce off-shell dependence into the vertex function which is not suppressed in the IMF. This leads to two possible choices for the meson energy: (i) the on-shell meson energy $E_M=\sqrt{m_M^2+k^2}$, or (ii) the off-shell meson energy, i.e. the difference between baryon energies E_N-E_B. While the second choice may be more ''natural'' in that the vertex structure is only due to baryonic currents [47,48], the first appears more compatible with TOPT in that the meson remains on-shell. In practice a number of authors [31,33] have used both prescriptions, and treated them as two different models.

We can gain some insight into the choice of meson energy if we recall that TOPT in the IMF is equivalent to light-cone perturbation theory (LCPT) [45,49,50]. In LCPT it is important to be aware of the light-cone singularities in the particle propagators. For spin-zero particles the Klein-Gordon propagator (in light-cone coordinates) is [49]

$$\Delta_F(x)=\frac{-i}{(2\pi)^3}\int d^2p_\perp\int_0^\infty\frac{dp^+}{2p^+}[\Theta(x^+)e^{-ip\cdot x}+\Theta(-x^+)e^{ip\cdot x}]. \tag{58}$$

The singularity at $p^+=0$ does not affect the light-cone behavior of the propagator, which is governed by the light-cone discontinuities $\Theta(\pm x^+)$. For particles of higher spin, the propagators all pick up terms proportional to

$$\delta(x^+)\frac{1}{(2\pi)^3}\int d^2p_\perp\int_{-\infty}^\infty\frac{dp^+}{2p^+}\exp[-i(p^-x^--\vec{p}_\perp\cdot\vec{x}_\perp)] \tag{59}$$

in addition to the terms proportional to $\Theta(\pm x^+)$. The term proportional to $\delta(x^+)$ is an instantaneous part of the propagator. This term can be absorbed into the regular propagator by replacing in the numerator of the diagrams in which the particle propagates over a single time interval, the momentum p associated with the line by

$$\tilde{p}=\Big(p^+,\sum_{\rm inc}p^--\sum_{\rm int}{}'p^-,\vec{p}_\perp\Big), \tag{60}$$

where $\sum_{\rm inc}$ sums over all the initial particles in the diagram and $\sum_{\rm int}{}'$ sums over all the particles in the intermediate state *except* the particle of interest [50]. Returning to TOPT in the IMF, we see that this is equivalent to choice (ii) for the meson energy, for nonscalar mesons. For spin-zero mesons there are no terms corresponding to instantaneous propagation (in light-cone coordinates), and the propagator is not adjusted. Hence for scalar and pseudoscalar mesons the correct meson energy is choice (i), i.e. the mesons are always treated as on-shell.

The vertex function $V_{IMF}^{\lambda\lambda'}(y,k_\perp^2)$ is calculated from the effective interaction Lagrangians (see Appendix B) which are usually employed in the meson exchange models [51]. Phenomenological vertex form factors $G_{BM}(y,k_\perp^2)$ are also introduced into Eq. (55) to describe the unknown dynamics of the fluctuation $N\to BM$ arising from the extended structure of hadrons. We use the exponential form factor

$$G_{BM}(y,k_\perp^2)=\exp\Big[\frac{m_N^2-m_{BM}(y,k_\perp^2)}{2\Lambda_{BM}^2}\Big], \tag{61}$$

with Λ_{BM} being a cutoff parameter, which is well defined in the model and provides a cutoff in both t and u (the four momentum squared of the intermediate baryon). The form factor satisfies the relation $G_{BM}(y,k_\perp^2)=G_{MB}(1-y,k_\perp^2)$. Using form factors introduces new parameters $\{\Lambda_{BM}\}$ into any calculation using the MCM, with each Fock state having (in principle) its own cutoff. However, the Jülich group [29] and Zoller [52] used high-energy particle production data to determine all the Λ_{BM} of interest, and found that the data could be described by two parameters: Λ_1 for octet baryons and pseudoscalar and vector mesons, and Λ_2 for decuplet baryons. The upper limits for these two parameters were determined to be about 1 GeV, which is fairly soft, and gives the probability of all Fock states totalling about 40%. Melnitchouk, Speth, and Thomas [28] found a good fit to both the violation of the Gottfried sum rule [24] and the observed ratio of $\bar{d}(x)/\bar{u}(x)$ from the E866 experiment [25] using values $\Lambda_1=0.80$ GeV and $\Lambda_2=1.00$ GeV, and we shall use these values of the cutoffs in this work.

The Fock states we consider are $|N\pi\rangle$, $|N\rho\rangle$, $|\Delta\pi\rangle$, and $|\Delta\rho\rangle$. The coupling constants and probabilities for each of these states in the nucleon wave function are shown in Tables I and II. The effect of increasing one or both cutoffs is to increase the probability for the states controlled by the cutoff, and correspondingly decrease the probability of finding the bare nucleon. Also the probability for higher mass Fock states increases faster with the cutoff than the

TABLE I. Strong coupling constants used in this work.

$\frac{g_{NN\pi}^2}{4\pi}$	$\frac{f_{N\Delta\pi}^2}{4\pi^2}$	$\frac{g_{NN\rho}^2}{4\pi}$	$f_{NN\rho}$	$\frac{f_{N\Delta\rho}^2}{4\pi}$
13.6	12.3 GeV^{-2}	0.84	$6.1g_{NN\rho}$	20.45 GeV^{-2}

TABLE II. Meson cloud model cutoff parameters and probabilities. Z is the wave function renormalization $Z = (1 + \sum_{BM} P_{BM})^{-1}$. In this paper we have used $\Lambda_1 = 0.8$ GeV and $\Lambda_2 = 1.0$ GeV. We also display the probabilities obtained using the cutoffs of the Jülich group [29].

Λ_1 (GeV)	Λ_2 (GeV)	$P_{N\pi}$	$P_{\Delta\pi}$	$P_{N\rho}$	$P_{\Delta\rho}$	Z
0.8	1.0	0.132	0.118	0.015	0.025	0.775
1.0	1.0	0.252	0.118	0.106	0.025	0.666

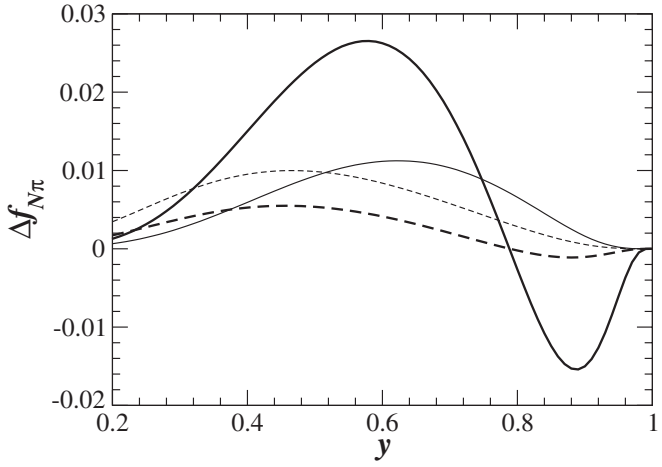

FIG. 3. Fluctuation functions for $N \to N\pi$ with N being struck. The thick solid and dashed curves are for Δf_{1L} and Δf_{2L}, respectively. The thin solid and dashed curves stand for $10\Delta f_{1T}$ and $100\Delta f_{2T}$, respectively.

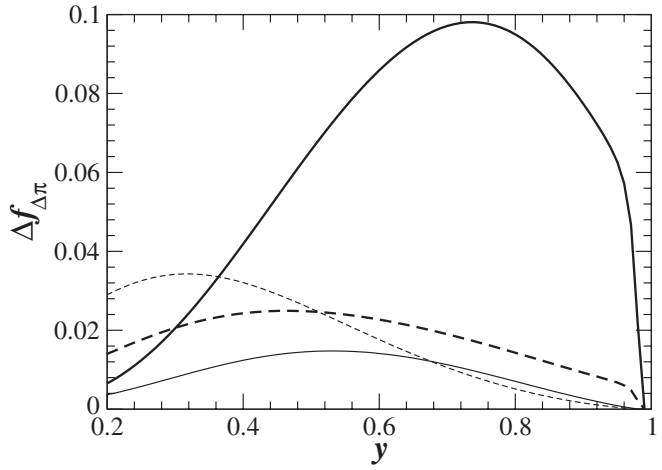

FIG. 4. Fluctuation functions for $N \to \Delta\pi$ with Δ being struck. The thick solid and dashed curves are for Δf_{1L} and Δf_{2L}, respectively. The thin solid and dashed curves stand for $10\Delta f_{1T}$ and $100\Delta f_{2T}$, respectively. $\Delta f_{1(2)L(T)} = \Delta f^{(3/2)(1/2)}_{1(2)L(T)} + 3\Delta f^{(3/2)(3/2)}_{1(2)L(T)}$.

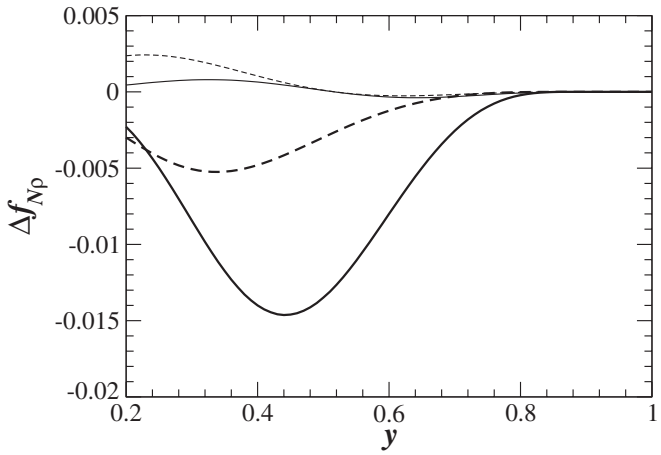

FIG. 5. Fluctuation functions for $N \to N\rho$ with N being struck. The thick solid and dashed curves are for Δf_{1L} and Δf_{2L}, respectively. The thin solid and dashed curves stand for $10\Delta f_{1T}$ and $100\Delta f_{2T}$, respectively.

probability for lower mass states, so increasing e.g. Λ_1 increases the ratio of $|N\rho\rangle$ states to $|N\pi\rangle$ states. The contributions from Fock states involving higher invariant mass squared are very small, at most a few percent of the contributions from the states we consider here. In Figs. 3–8 we show the fluctuation functions $f_{NBM}(y)$ for each of the Fock states. In each of these calculations we take $x = 0.2$ and $Q^2 = 2.5$ GeV^2, i.e. $\gamma^2 = 0.056$. In general, we see that the longitudinal functions $\Delta f_{1L,2L}$ are much larger that the transverse functions $\Delta f_{1T,2T}$. This means that the contributions to g_1 of the nucleon coming from g_2 of the struck hadron will be small, whereas the kinematic contributions to g_2 of the nucleon from g_1 of the struck hadron should not be ignored as they will generally be larger than the contributions coming from g_2 of the Fock state hadrons. We

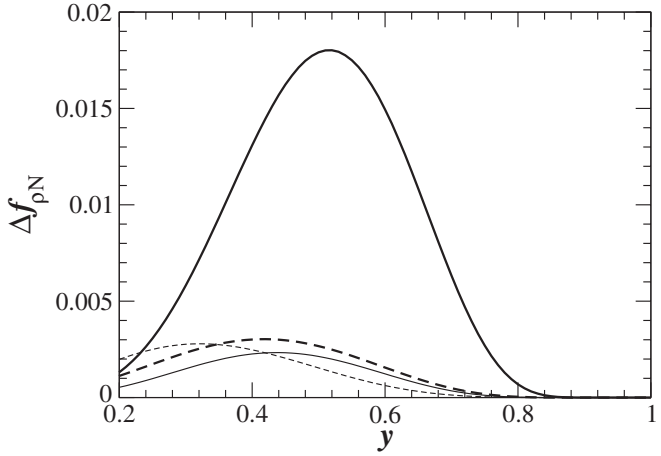

FIG. 6. Fluctuation functions for $N \to N\rho$ with ρ being struck. The thick solid and dashed curves are for Δf_{1L} and Δf_{2L}, respectively. The thin solid and dashed curves stand for $10\Delta f_{1T}$ and $100\Delta f_{2T}$, respectively.

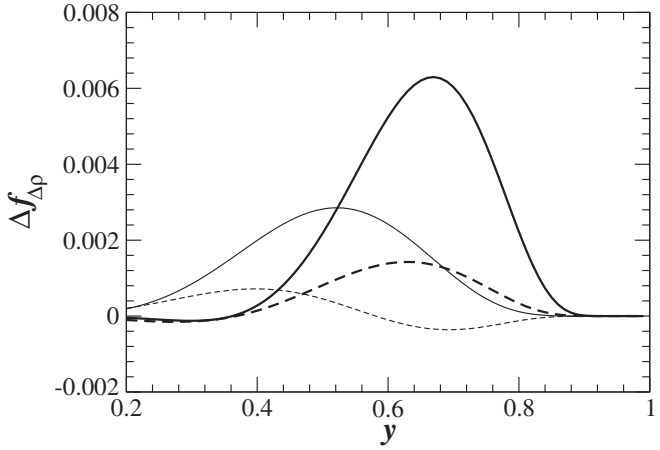

FIG. 7. Fluctuation functions for $N \to \Delta\rho$ with Δ being struck. The thick solid and dashed curves are for Δf_{1L} and Δf_{2L}, respectively. The thin solid and dashed curves stand for $10\Delta f_{1T}$ and $100\Delta f_{2T}$, respectively. $\Delta f_{1(2)L(T)} = \Delta f^{(3/2)(1/2)}_{1(2)L(T)} + 3\Delta f^{(3/2)(3/2)}_{1(2)L(T)}$.

also observe that the fluctuation functions arising from $|\Delta\pi\rangle$ states are generally much larger than those of the other Fock states we consider. Amplitudes with the Δ having $s = 3/2$ are particularly important. We therefore expect that the $|\Delta\pi\rangle$ fluctuation will play a very important role in the MCM contributions to the spin structure functions. Fluctuation functions involving ρ mesons should not be neglected either, as these are of similar size to the $|N\pi\rangle$ fluctuation functions.

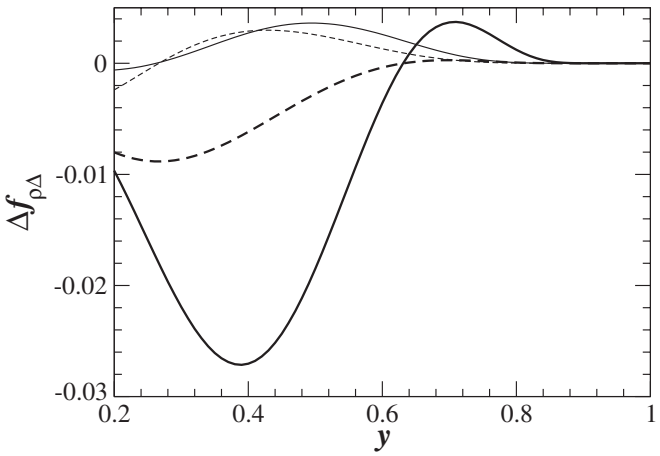

FIG. 8. Fluctuation functions for $N \to \Delta\rho$ with ρ being struck. The thick solid and dashed curves are for Δf_{1L} and Δf_{2L}, respectively. The thin solid and dashed curves stand for $10\Delta f_{1T}$ and $100\Delta f_{2T}$, respectively. $\Delta f_{1(2)L(T)} = \Delta f^{(3/2)(1/2)}_{1(2)L(T)} + 3\Delta f^{(3/2)(3/2)}_{1(2)L(T)}$.

V. POLARIZED STRUCTURE FUNCTIONS OF BARE HADRONS

To use the meson cloud model, we need to know the polarized structure functions of all the baryons and mesons in the Fock expansion of the nucleon wave function. At present the only polarized structure functions that are known experimentally are those of the proton and neutron (apart from the trivial case of the pseudoscalar or scalar mesons). It would appear unlikely that the structure functions of the ρ mesons and the Δ baryons, which are the most important polarized cloud constituents, will be measured in the near future. Our approach therefore is to estimate all the structure functions we require, including those of the nucleons, using the MIT bag model [53,54] and the methods developed by the Adelaide group [30,55] and ourselves [34,56]. This approach gives a reasonable description of the unpolarized structure functions of the nucleons when compared to experimental data.

In the bag model the dominant contributions to the parton distribution functions of a hadron in the medium-x range come from intermediate states with the lowest number of quarks, so the intermediate states we consider contain one quark (or antiquark) for the mesons and two quarks for the baryons. Following [55] we can write these contributions as

$$q^{\uparrow\downarrow}_{h,f}(x) = \frac{M_h}{(2\pi)^3}\sum_m \langle\mu|P_{f,m}|\mu\rangle \int d\mathbf{p}_n \frac{|\phi_i(\mathbf{p}_n)|^2}{|\phi_j(\mathbf{0})|^2} \times \delta(M_h(1-x) - p_n^+)|\tilde{\Psi}^{\uparrow\downarrow}_{+,f}(\mathbf{p}_n)|^2, \quad (62)$$

where M_h is the hadron mass, "+" components of momenta are defined by $p^+ = p^0 + p^3$, and $\mathbf{p}_n$ is the 3-momentum of the intermediate state. $\tilde{\Psi}$ is the Fourier transform of the MIT bag ground state wave function $\Psi(\mathbf{r})$, and $\phi_m(\mathbf{p})$ is the Fourier transform of the Hill-Wheeler overlap function between m-quark bag states:

$$|\phi_m(\mathbf{p})|^2 = \int d\mathbf{R}\, e^{-i\mathbf{p}\cdot\mathbf{R}}\left[\int d\mathbf{r}\Psi^\dagger(\mathbf{r}-\mathbf{R})\Psi(\mathbf{r})\right]^m. \quad (63)$$

In Eq. (62) we take $i = 1$, $j = 2$ for the mesons and $i = 2$, $j = 3$ for the baryons. The matrix element $\langle\mu|P_{f,\lambda}|\mu\rangle$ appearing in Eq. (62) is the matrix element of the projection operator $P_{f,m}$ onto the required flavor f and helicity λ for the SU(6) spin-flavor wave function $|\mu\rangle$ of the hadron under consideration.

The input parameters in the bag model calculations are the bag radius R, the mass of the quark (antiquark) m_q for which the parton distribution is calculated, the mass of the intermediate state m_n, and the bag scale μ^2—at this scale the model is taken as a good approximation to the valence structure of the hadron. The natural scale for the model is set by the typical quark $k_\perp$, which is around 0.4 GeV. In Table III we list the values for these parameters adopted in this work. These values have previously been shown to give a good description of the unpolarized nucleon parton

TABLE III. Input parameters for the bag model calculation of bare structure functions.

	R (fm)	m_q (MeV)	m_n (MeV)	μ^2 (GeV^2)
N	0.8	0	800	0.23
ρ	0.7	0	425	0.23

distributions [30] and also of the meson distributions [34]. After calculating the hadron structure functions at the bag scale μ^2, we evolve them using next-to-leading order (NLO) evolution [57] to the scale of $Q^2 = 2.5$ GeV^2 where the HERMES results for g_1^p [4] and g_1^n [6] are available. While NLO evolution from the bag scale appears stable, it would be of interest to compare with next-to-next-to-leading order (NNLO) evolution, as it is known that LO evolution does not give very good results for this procedure [58]. Unfortunately, the necessary NNLO coefficient functions and anomalous dimensions for spin dependent structure functions and parton distributions have not all been calculated at this time.

The calculated polarized structure functions $g_1^p(x)$ and $g_1^n(x)$ agree reasonably well with experimental data at medium and large x, however they do not give a good description of the low x data (see the thin solid curves in Figs. 11 and 12). This discrepancy may well arise because our bag model calculations cannot estimate the polarized gluon distribution $\Delta g(x)$, which is believed to play an important role in the observed spin of the nucleons [59]. We can add a phenomenological $\Delta g(x)$,

$$\Delta g(x) = N_g(1 - x)^\alpha, \tag{64}$$

to our calculated structure functions, where global analyses of polarized deep inelastic scattering data suggest α should be in the range of 7–10 [60]. In this work we use a value of $\alpha = 10$, however we have found that the calculated structure functions are not very sensitive to the value of α. We normalize the polarized gluon distribution so that the contribution of polarized gluons to the first moment of g_1^p (Ellis-Jaffe sum rule) and g_1^n is -0.05, which gives theoretical moments that are in agreement with experiment. The structure functions g_1 for the bare proton, neutron, Δ^+ and ρ are given in Fig. 9. We have not taken account of any possible topological contributions to the singlet axial charge $g_A^{(0)}$, which can also contribute to $g_1(x)$ at $x = 0$ [61]. As our procedure gives a reasonable description of the observed $g_1^p(x)$ and $g_1^n(x)$, especially once MCM contributions have been added (see below), there appears little need to add an extra phenomenological term to the bare structure functions.

The structure functions g_2 for the bare hadrons are estimated via the Wandzura-Wilczek relation [62] which is obtained by considering only twist-2 contributions to g_1 and g_2,

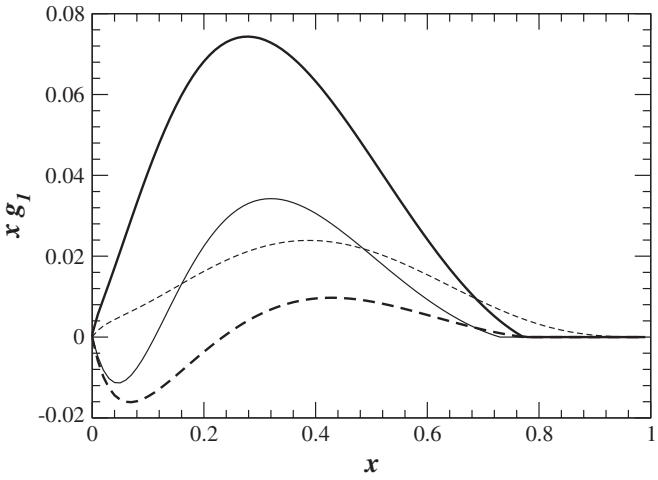

FIG. 9. "Bare" structure functions $xg_1(x)$ of the nucleons, delta baryons and ρ meson at $Q^2 = 2.5$ GeV^2. The thick solid and dashed lines are for the proton and neutron, respectively. The thin solid line is for the Δ^+ baryon and the thin dashed line is for the ρ meson.

$$g_2^{WW}(x, Q^2) = -g_1(x, Q^2) + \int_x^1 \frac{dy}{y} g_1(y, Q^2). \tag{65}$$

We also note that previous bag model studies of $g_2(x)$ [14,15,56] accord reasonably well with the experimental data.

VI. NUMERICAL RESULTS AND DISCUSSIONS

We show our results for the MCM contributions to $g_1^p(x)$ and $g_2^p(x)$ at $Q^2 = 2.5$ GeV^2 in Fig. 10. As expected, the dominant contributions to g_1^p are the longitudinal contributions of the form $\Delta f_{iL} \otimes g_i$, while the transverse contributions are fairly small at this scale. For g_2^p the transverse contributions are similar in size to the longitudinal contributions, but tend to be opposite in sign, which makes the overall MCM contribution to g_2^p smaller than for g_1^p. We also show the contribution from the $|N\pi\rangle$ portion of the MCM wave function. While important, it is clear that taking into account only this part of the wave function does not give a good indication of the total MCM contribution to the spin dependent structure functions. The Δ baryon, especially the $s = 3/2$ component, plays an important role and should not be ignored.

In Figs. 11 and 12 we compare theoretical calculations for g_1^p and g_1^n with recent experimental measurements from HERMES Collaboration [4,6]. The calculation of $g_1^n(x)$ agrees very well with the data, but the agreement is less impressive in the case of $g_1^p(x)$, where the calculated structure function is significantly smaller than the data points in the region $x > 0.3$, and the peak of the calculated structure function occurs near $x = 0.3$. As can be seen in Fig. 11, the fit to the experimental data is considerably improved by including both the polarized gluon distribution and meson cloud effects. It is known [30,63] that the

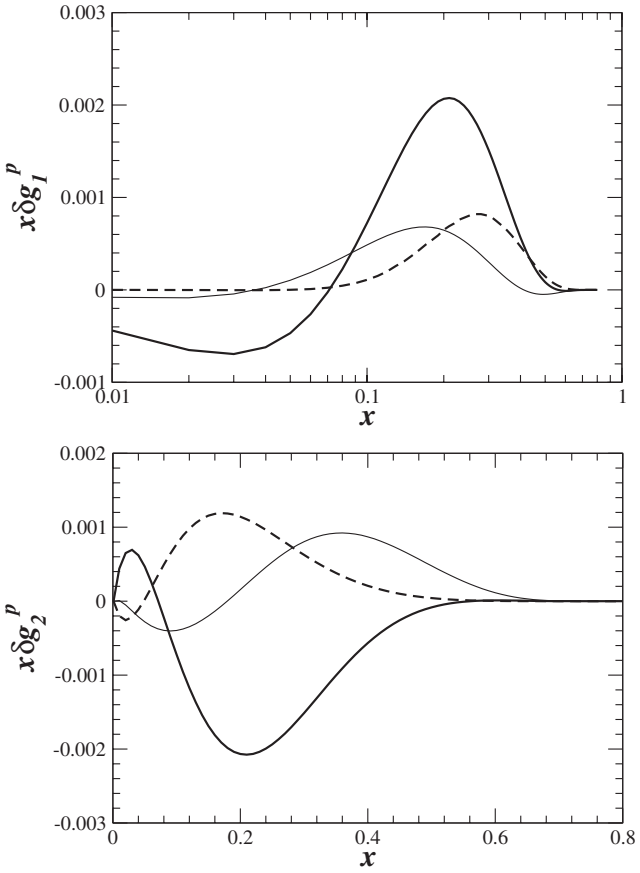

FIG. 10. Meson cloud model contributions to $g_1^p(x)$ and $g_2^p(x)$ at $Q^2 = 2.5$ GeV^2. The thick lines are the total longitudinal contributions to the structure functions. The thick dashed lines are the total transverse contributions to the structure functions [multiplied by 10 in the case of $g_{1T}(x)$]. The thin lines show the total contribution of the $|N\pi\rangle$ Fock state to the structure functions [multiplied by 5 in the case of $g_2(x)$].

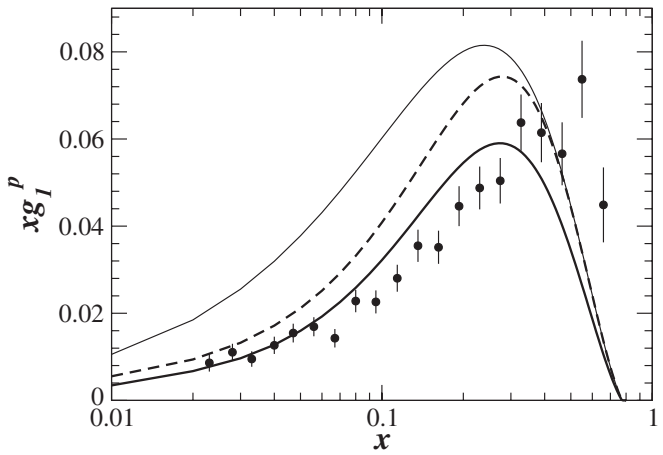

FIG. 11. Spin dependent structure functions xg_1^p at $Q^2 = 2.5$ GeV^2. The thin solid curve is the bag model calculation. The thick dashed curve is the bag model calculation plus contributions from the polarized gluon. The thick solid curve is the total result in the MCM calculations. The HERMES data are taken from [4].

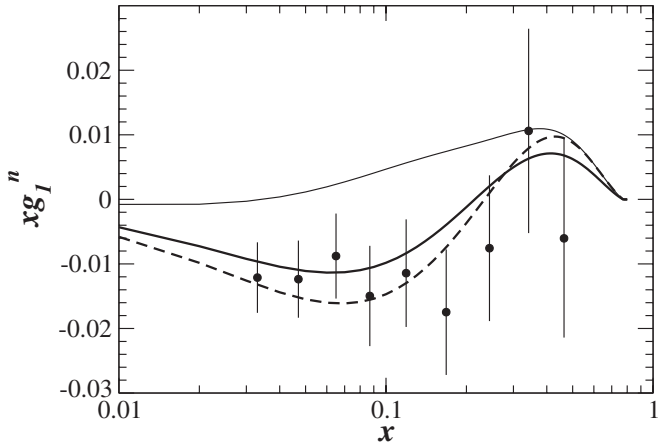

FIG. 12. As in Fig. 11 but for xg_1^n. The HERMES data are taken from [6].

meson cloud lowers the bag model calculation for g_1^p over the entire range of x since the angular momentum of the meson cloud carries some of the spin of the nucleon. However these calculations overestimate $g_1^p(x)$ in the region $x < 0.1$ and give results with much smaller magnitude than the experimental data for $g_1^n(x)$ in the region $x < 0.2$. Including the polarized gluon distribution significantly improves the fit to the experimental data. The importance of these polarized gluon contributions is more obvious in the calculation of the structure function g_1^n. Without these contributions our theoretical calculations are not able to reproduce the shape of the experimental data. We note that the magnitude of the polarized gluon distribution we use is determined only by the Ellis-Jaffe sum rule, and we have not attempted to change the shape of the distribution to improve the agreement with the data. A harder polarized gluon distribution would reduce g_1^p even more at large x. Another factor which affects the quality of our fit to the data at large x is the difficulty the bag model calculation of structure functions has in this region because of the non-relativistic projection used to form momentum eigenstates [55], which results in the calculated distributions being systematically smaller than the data.

The values for the Ellis-Jaffe sum rule for the proton and neutron are found to be 0.120 and -0.027, respectively, which are close to the experimental values at this scale of $\int_{0.021}^{0.85} g_1^p(x)dx = 0.122 \pm 0.003(\text{stat.}) \pm 0.010(\text{sys.})$ [4] and $-0.037 \pm 0.013(\text{stat.}) \pm 0.005(\text{sys.}) \pm 0.006(\text{extrap.})$ [6]. The Bjorken sum rule is found to be 0.147 which is close to the experimental value, and can also be compared with the theoretical value calculated to $O(\alpha_S^3)$ [64] of 0.173. This is consistent with the value of g_A calculated in the bag model being 10% smaller than the experimental value. In this work, the structure functions have been calculated by considering only the contributions from the valence partons. In the MCM, the polarized antiquark distributions $\Delta\bar{u}(x)$ and $\Delta\bar{d}(x)$ are found to be rather small [34,65]. However, Pauli blocking effects [32,66] may be of

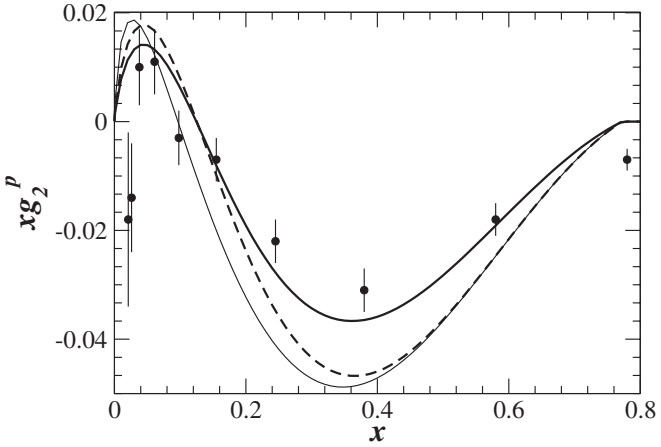

FIG. 13. Spin dependent structure functions xg_2^p at $Q^2 = 2.5$ GeV^2. The thin solid curve is the bag model calculation. The thick dashed curve is the bag model calculation plus contributions from the polarized gluon. The thick solid curve is the total result in the MCM calculations. The data are taken from SLAC-E155 [9] and 0.8 GeV$^2 < Q^2 <$ 8.2 GeV^2.

similar size in the polarized distributions as in the unpolarized distributions [28], and could contribute 5%–10% to the observed value of the Bjorken sum rule.

Now we turn our attention to the calculations for the structure functions $g_2(x)$. The results are presented in Figs. 13 and 14 for the proton and neutron, respectively, along with experimental data from E99-177, E97-103, and E155 Collaborations. The agreement between theoretical calculations and experimental measurements for the proton in the region $0.05 < x < 0.7$ is very good. The calculations for g_2^n are consistent with the recent precision measurement at JLab for $x \simeq 0.2$, although experimental information on the x-dependence of $g_2^n(x)$ is not conclusive due to large error bars. Once again we find that including the polarized gluon contribution is crucial to the calculations for the region $x < 0.2$, especially for the calculation of

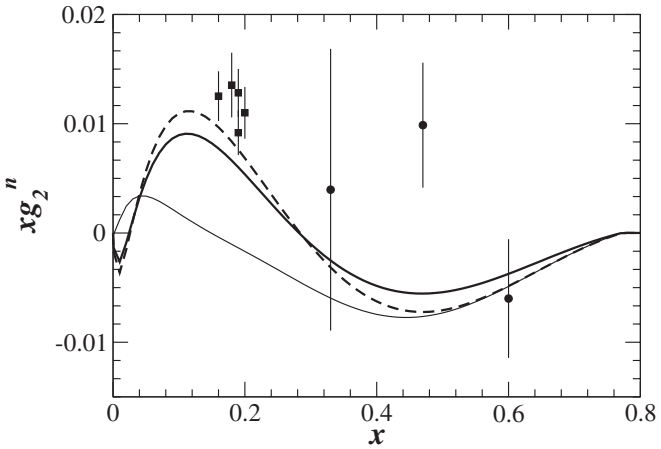

FIG. 14. As in Fig. 11 but for xg_2^n. The data are taken from Jefferson Lab experiments [11,12] and 0.57 GeV$^2 < Q^2 <$ 4.83 GeV^2.

TABLE IV. Comparison of our calculations with experiment for the moments of the g_2 structure functions, where $\mathcal{M}_n[g_2] = \int_0^1 x^n g_2(x) dx$.

	$\mathcal{M}_2[g_2^p] \times 10^3$	$\mathcal{M}_4[g_2^p] \times 10^3$	$\mathcal{M}_6[g_2^p] \times 10^3$
This work	-5.13	-1.14	-0.33
Experiment [9]	$-7.2 \pm 0.5 \pm 0.3$		
	$\mathcal{M}_2[g_2^n] \times 10^3$	$\mathcal{M}_4[g_2^n] \times 10^3$	$\mathcal{M}_6[g_2^n] \times 10^3$
This work	-0.564	-0.203	-0.067
Experiment [8]	3.3 ± 6.5		

$g_2^n(x)$. The cloud mesons can have a dramatic effect on the calculations for the structure functions $g_2^{p,n}$, especially in the region $0.1 < x < 0.4$. For g_2^n in the region of $x \sim 0.1$ the cloud contributions are comparable in magnitude with the bare contributions.

The close agreement between our calculations and the experiments implies that any twist three portion of $g_2(x)$ is rather small. We note that experimental data from E155 [9] is compatible, within 2 standard deviations, with there being no twist three contribution to the structure functions. If precision experiments at low values of Q^2 also show no firm evidence for twist three contributions to g_2, this will provide a new challenge for model builders, as it is expected that higher twist parts of the structure functions will be of similar size to leading twist contributions at the model scale [56]. We give our results for the first few moments of g_2^p and g_2^n, along with the experimental estimates of these moments in Table IV. The disagreement between our value of the second moment of g_2^p and that of E155 is largely due to the data point at $x = 0.78$ which gets a large weighting in the calculation of the moment.

VII. SUMMARY

We have used the meson cloud model to calculate the spin dependent structure functions $g_1(x)$ and $g_2(x)$ of the proton and neutron. An important part of this calculation is the use of bare structure functions of the hadrons in the model calculated in the MIT bag model, with the addition of an extra polarized gluon term, which gives good agreement with the observed value of the lowest moment of g_1^p (Ellis-Jaffe sum rule).

We included in our calculations the full effects of kinematic terms that arise at finite Q^2 because the spin vector of the struck hadron is not parallel with the spin vector of the initial nucleon. This leads to three or more additional contributions to each spin dependent structure function for each hadron species included in the model nucleon wave function. While these contributions vanish in the Bjorken limit, they can make a substantial proportion of the observed structure functions at finite Q^2, and are particularly important for describing the neutron structure functions. We note that these contributions have the same form as expected for target mass corrections [36] and

should not be confused with genuine higher twist contributions to the structure functions, which arise from new operators involving quark-gluon correlators [56,67]. As the quality of data on neutron structure functions improves, it will be interesting to compare the behavior of the structure functions as a function of Q^2 with that predicted by the MCM. We have not done this here, as most of the data is at fairly low x, and the Q^2 variation in this kinematic region is quite small.

We have considered the effects of possible interference between intermediate states containing different hadrons, which can contribute to the spin dependent parts of the DIS cross section. Our analysis shows that for the most part these terms cannot affect the observed structure functions or parton distributions. It is possible that states involving higher spins, e.g. $|\Delta\rho\rangle$, can give interference contributions. The difficulties in calculating the dynamics of the relevant vertices are formidable, however these terms are suppressed in the MCM owing to their high mass, so we have ignored these contributions in this work.

Our calculations of the spin dependent structure functions show good agreement with the experimental data. We see significant corrections to the structure functions calculated using the bag model arising both from the inclusion of a polarized gluon distribution and from the cloud contributions. In both cases these improve the agreement with the experimental data. Our calculations of $g_2(x)$ includes only the Wandzura-Wilczek term, which gives the twist two portion of the structure function.

There is a further spin dependent structure function of the nucleon, which we have not discussed in this paper. This is the transversity distribution $h_1(x)$, which measures the distribution of transversely polarized quarks in a transversely polarized nucleon. In the nonrelativistic limit $h_1(x) = g_1(x)$, so a measurement of h_1 can tells us about the importance of relativistic effects in the quark wave function. We will be extending our calculations to the transversity distribution of the proton and neutron, where we expect that meson cloud model effects will affect significantly the observed structure functions.

ACKNOWLEDGMENTS

We thank Tony Thomas for helpful comments and encouragement. This work was partially supported by the Marsden Fund of the Royal Society of New Zealand and the Foundation for Research, Science and Technology. A. S. acknowledges the hospitality and support of the Institute for Particle Physics Phenomenology, Durham University, where portions of this work were done.

APPENDIX A: BARYON AND MESON MOMENTUM DISTRIBUTIONS

We reproduce here the results for the general form of the baryon and meson momentum distributions $f^{\lambda}_{1,2L,T}(y)$ as given by Kumano and Miyama [33] for spin 1 mesons. As we have noted above, these results also hold for spin $1/2$ baryons and can be generalized to spin $3/2$ baryons. First, we note that the portion of the integrand of Eq. (16) that depends on J_{NMB}, the NMB vertex times the propagator of the struck hadron, may be written as a sum of an unpolarized, a longitudinal and a transverse part:

$$\frac{|\vec{p}_N|}{(2\pi)^3} y \frac{\partial y'}{\partial y} \sum_{\lambda'} |J_{NBM}|^2 = C_0^{\lambda} + \lambda_N C_L^{\lambda} + \tau_N \cos\phi C_T^{\lambda}, \tag{A1}$$

where ϕ is the angle between $\vec{k}_\perp$ and $\vec{s}_N^{\top}$, $\vec{k}_\perp \cdot \vec{s}_N^{\top} = |\vec{k}_\perp| \tau_N \cos\phi$, and λ labels the helicity of the struck hadron. We find that the unpolarized part is such that $C_0^{-\lambda} = C_0^{\lambda}$, so any contribution arising from this part will cancel itself when we compute Δf using Eq. (21). Therefore we will ignore any contributions from C_0^{λ} in the following. Performing the integration over ϕ then gives Eq. (20) with the hadron momentum distributions given by

$$f^{\lambda}_{1L,T}(y) = \int_0^{(k_\perp^2)_m} d\vec{k}_\perp^2 \, r^{\lambda}_{1L,T}(\vec{k}_\perp^2, m) \tag{A2}$$

$$f^{\lambda}_{2L,T}(y) = \int_0^{(k_\perp^2)_m} d\vec{k}_\perp^2 \, r^{\lambda}_{2L,T}(\vec{k}_\perp^2, m), \tag{A3}$$

where m is the mass of the struck hadron and the integrands $r^{\lambda}_{1,2i}$ are given by

$$r^{\lambda}_{1L}(\vec{k}_\perp^2, m) = 2\pi C_L^{\lambda} \left[1 + \frac{k_\perp^2}{y y' m_N^2} \left(\sqrt{1+\gamma^2} - 1 \right) \right] \tag{A4}$$

$$r^{\lambda}_{1T}(\vec{k}_\perp^2, m) = -\gamma^2 \pi C_T^{\lambda} \frac{k_\perp}{y m_N} \tag{A5}$$

$$r^{\lambda}_{2L}(\vec{k}_\perp^2, m) = -\gamma^2 \pi C_L^{\lambda} \frac{m^2}{y^2 m_N^2} \tag{A6}$$

$$r^{\lambda}_{2T}(\vec{k}_\perp^2, m) = \gamma^2 \pi C_T^{\lambda} \frac{k_\perp m^2}{y^2 y' m_N^3} \left(\sqrt{1+\gamma^2} - 1 \right). \tag{A7}$$

We note that we have changed the signs of f_{1T} and f_{2L} from those of [33], as this is more consistent with the notation we use below for the spin $3/2$ baryon momentum distributions In the Bjorken limit only f_{1L} remains nonzero. By combining the longitudinal $\lambda_N = 1 (\tau_N = 0)$ with the transverse $\lambda_N = 0$ $(\tau_N = 1)$ amplitude in Eq. (20), and defining the functions

$$\Delta f^{j}_{1,2L,T}(y) = f^{\lambda=+j}_{1,2L,T}(y) - f^{\lambda=-j}_{1,2L,T}(y) \tag{A8}$$

with j the spin of the struck hadron, we can obtain the separate contributions to the nucleon g_1 and g_2 structure functions:

$$\delta g_1(x,Q^2) = \frac{1}{1+\gamma^2}\int_x^1 \frac{dy}{y}\sum_{i=1,2}[\Delta f_{iL}^j(y) - \Delta f_{iT}^j(y)]g_i^j\left(\frac{x}{y},Q^2\right) \quad \text{(A9)}$$

$$\delta g_2(x,Q^2) = -\frac{1}{1+\gamma^2}\int_x^1 \frac{dy}{y}\sum_{i=1,2}\left[\Delta f_{iL}^j(y) + \frac{\Delta f_{iT}^j(y)}{\gamma^2}\right]g_i^j\left(\frac{x}{y},Q^2\right). \quad \text{(A10)}$$

The momentum distributions for spin $3/2$ baryons follow a similar pattern to those above. In this case the distributions also have to be labeled by $h = \frac{1}{2}, \frac{3}{2}$ with $\lambda = \pm h$. We obtain

$$f_{1L,T}^{(3/2)\lambda}(y) = \int_0^{(k_\perp^2)_m} d\vec{k}_\perp^2\left[\frac{14-2\omega^2}{15}r_{1L,T}^\lambda(\vec{k}_\perp^2,m) + \frac{4}{15}r_{2L,T}^\lambda(\vec{k}_\perp^2,m)\right] \quad \text{(A11)}$$

$$f_{2L,T}^{(3/2)\lambda}(y) = \int_0^{(k_\perp^2)_m} d\vec{k}_\perp^2\,\frac{18-2\omega^2}{15}r_{2L,T}^\lambda(\vec{k}_\perp^2,m) \quad \text{(A12)}$$

$$f_{1L,T}^{(1/2)\lambda}(y) = \int_0^{(k_\perp^2)_m} d\vec{k}_\perp^2\left[\frac{6+2\omega^2}{5}r_{1L,T}^\lambda(\vec{k}_\perp^2,m) - \frac{4}{5}r_{2L,T}^\lambda(\vec{k}_\perp^2,m)\right] \quad \text{(A13)}$$

$$f_{2L,T}^{(1/2)\lambda}(y) = \int_0^{(k_\perp^2)_m} d\vec{k}_\perp^2\,\frac{2+2\omega^2}{5}r_{2L,T}^\lambda(\vec{k}_\perp^2,m). \quad \text{(A14)}$$

Now defining

$$\Delta f_{1,2L,T}^{(3/2)l}(y) = l[f_{1,2L,T}^{l\lambda=+l}(y) - f_{1,2L,T}^{l\lambda=-l}(y)], \quad \text{(A15)}$$

the contributions to the structure functions become

$$\delta g_1(x,Q^2) = \frac{1}{1+\gamma^2}\int_x^1 \frac{dy}{y}\sum_{i=1,2}\sum_{h=1/2,3/2}[\Delta f_{iL}^{(3/2)h}(y) - \Delta f_{iT}^{(3/2)h}(y)]g_i^{(3/2)h}\left(\frac{x}{y},Q^2\right) \quad \text{(A16)}$$

$$\delta g_2(x,Q^2) = -\frac{1}{1+\gamma^2}\int_x^1 \frac{dy}{y}\sum_{i=1,2}\sum_{h=(1/2),(3/2)}\left[\Delta f_{iL}^{(3/2)h}(y) + \frac{\Delta f_{iT}^{(3/2)h}(y)}{\gamma^2}\right]g_i^{(3/2)h}\left(\frac{x}{y},Q^2\right). \quad \text{(A17)}$$

APPENDIX B: CALCULATION OF $N-\Delta$ INTERFERENCE TERMS

As an example of the general technique for calculating the vertex functions in the MCM, and more specifically how to calculate interference terms, we present the calculation of the terms for interference between $|N\pi\rangle$ and $|\Delta\pi\rangle$ states, where the pion is the spectator. We start from the interaction Lagrangians for the two vertices [29,48,51]

$$\mathcal{L}_1 = ig_{NN\pi}\bar{\psi}\gamma_5\pi\psi \quad \text{(B1)}$$

$$\mathcal{L}_2 = f_{N\Delta\pi}\bar{\psi}\partial_\mu\pi U^\mu + \text{H.c.}, \quad \text{(B2)}$$

where $U^\mu(p,s)$ is the Rarita-Schwinger spinor for the spin $3/2$ field. These give the required vertices in the numerators of $J_{NN\pi}$ and $J_{N\Delta\pi}$, whereas the denominators will be given by the propagators of the nucleon and Δ. respectively. Standard techniques then give us that $\mathcal{R}[J_{N\Delta\pi}J_{NN\pi}^*]$ is proportional to the trace of

$$\tfrac{1}{2}[u(p,s)\bar{u}(p,s)](\gamma_5 E^\mu(k_1,s_1)\bar{u}(k_2,s_2) - u(k_2,s_2)\bar{E}^\mu(k_1,s_1)\gamma_5)p'_\mu, \quad \text{(B3)}$$

where $E^\mu(k_1,s_1)$ is the positive energy spin $3/2$ spinor, which is a linear combination of Dirac spinors of positive and negative helicity with polarization vectors ϵ^μ for longitudinal and left or right circular polarization in the moving frame. We note that the nucleon and Δ in the intermediate states do not have identical momentum or spin 4-vectors, which may have been previously overlooked in earlier calculations. This fact makes the interference calculations much more difficult than the usual noninterference terms as $E^\mu(k_1,s_1)\bar{u}(k_2,s_2)$ cannot be written as a propagator, but requires careful evaluation. We also note that our calculation adds together two contributions depending on whether the initial MCM state is $|N\pi\rangle$ or $|\Delta\pi\rangle$. As these two are Hermitian conjugates, the final result should be real, which acts as a check that we have correctly accounted for all phase factors.

It is easiest to do the calculation in two parts, corresponding to the $\lambda = \pm 1/2$ helicities of the intermediate state hadrons. For the coefficients $C_{0,L,T}^\lambda$ of Eq. (53) we obtain

$$C_0^+(\phi) = C_0^-(\phi) = \frac{k_\perp^2(m_N+m_\Delta)}{4\sqrt{6}m_N\sqrt{m_N m_\Delta}y'^2}\cos\phi \quad \text{(B4)}$$

$$C_L^+(\phi) = -C_L^-(\phi) = \frac{k_\perp^2(m_N(1-2y')-m_\Delta)}{4\sqrt{6}m_N\sqrt{m_N m_\Delta}y'^2}\cos\phi \quad \text{(B5)}$$

and

$$C_T^+(\phi) = -C_T^-(\phi)$$
$$= \frac{(y'-1)(y'm_N + m_\Delta)k_\perp}{4\sqrt{6}y'^2\sqrt{m_N m_\Delta}} - \frac{k_\perp^3}{4\sqrt{6}y'^2 m_N\sqrt{m_N m_\Delta}} \times \cos(2\phi) + \frac{(m_N + m_\Delta)(k_\perp^2 + y'^2 m_\pi^2 - (y'-1)^2 m_\Delta^2)k_\perp}{4\sqrt{6}(y'-1)y'^2(m_N m_\Delta)^{3/2}} \times \sin(\phi). \quad \text{(B6)}$$

These coefficients now must be multiplied by coefficients $A_{1,2}^{N\Delta}$, $\tilde{A}_{1,2}^{N\Delta}$ from Eq. (46), all of which have the structure

$$A_i^{N\Delta} = a_i^L \lambda_N + a_i^T \tau_N \cos\phi \quad \text{(B7)}$$

and similarly for $\tilde{A}_{1,2}^{N\Delta}$, where λ_N and τ_N refer to the polarization of the parent nucleon. The functions $r_{1,2L,T}^\lambda$ (and their analogous $\tilde{r}_{1,2L,T}^\lambda$) are then given by

$$r_{iL}^\lambda = \int_0^{2\pi} d\phi a_i^L C_L^\lambda \quad \text{(B8)}$$

$$r_{iT}^\lambda = \int_0^{2\pi} d\phi a_i^T C_T^\lambda \cos\phi \quad \text{(B9)}$$

while any contribution to the unpolarized cross section will be proportional to

$$\int_0^{2\pi} d\phi [C_0^+ + C_0^-]. \quad \text{(B10)}$$

By inspection all these angular integrals are zero. Thus the interference between $|N\pi\rangle$ and $|\Delta\pi\rangle$ intermediate states makes no contribution to the observed structure functions. Similar arguments hold for the case of interference between $|N\pi\rangle$ and $|N\rho\rangle$ intermediate states.

[1] J. Ashman *et al.* (EMC Collaboration), Phys. Lett. B **206**, 364 (1988); J. Ashman *et al.*, Nucl. Phys. **B328**, 1 (1989).
[2] K. Abe *et al.* (E154 Collaboration), Phys. Rev. Lett. **79**, 26 (1997).
[3] B. Adeva (SMC Collaboration), Phys. Rev. D **58**, 112001 (1998).
[4] A. Airapetian *et al.* (HERMES Collaboration), Phys. Lett. B **442**, 484 (1998).
[5] B. Adeva *et al.* (SMC Collaboration), Phys. Rev. D **58**, 112001 (1998).
[6] K. Ackerstaff *et al.* (HERMES Collaboration), Phys. Lett. B **404**, 383 (1997).
[7] J. D. Bjorken, Phys. Rev. **148**, 1467 (1966); Phys. Rev. D **1**, 1376 (1970).
[8] K. Abe *et al.* (E143 Collaboration), Phys. Rev. D **58**, 112003 (1998).
[9] P. L. Anthony *et al.* (E155 Collaboration), Phys. Lett. B **553**, 18 (2003).
[10] K. Abe *et al.* (E154 Collaboration), Phys. Lett. B **404**, 377 (1997).
[11] X. Zheng *et al.* (Hall A Collaboration), Phys. Rev. C **70**, 065207 (2004).
[12] K. Kramer *et al.* (Hall A Collaboration), Phys. Rev. Lett. **95**, 142002 (2005).
[13] A. W. Schreiber, A. I. Signal, and A. W. Thomas, Phys. Rev. D **44**, 2653 (1991); A. W. Schreiber, P. J. Mulders, A. I. Signal, and A. W. Thomas, Phys. Rev. D **45**, 3069 (1992).
[14] X. Song and J. S. McCarthy, Phys. Rev. D **49**, 3169 (1994); **50**, 4718(E) (1994); X. Song, Phys. Rev. D **54**, 1955 (1996).
[15] M. Stratmann, Z. Phys. C **60**, 763 (1993).
[16] H. Weigel, L. P. Gamberg, and H. Reinhardt, Mod. Phys. Lett. A **11**, 3021 (1996); Phys. Rev. D **55**, 6910 (1997).
[17] D. I. Diakonov, V. Y. Petrov, P. V. Pobylitsa, M. V. Polyakov, and C. Weiss, Nucl. Phys. **B480**, 341 (1996); Phys. Rev. D **56**, 4069 (1997).
[18] M. Wakamatsu and T. Kubota, Phys. Rev. D **60**, 034020 (1999); M. Wakamatsu, Phys. Lett. B **487**, 118 (2000).
[19] J. W. Negele *et al.*, Nucl. Phys., Proc. Suppl. **B128**, 170 (2004).
[20] C. Adloff *et al.* (H1 Collaboration), Eur. Phys. J. C **6**, 587 (1999).
[21] M. Derrick *et al.* (Zeus Collaboration), Phys. Lett. B **384**, 388 (1996); S. Chekanov *et al.* (Zeus Collaboration), Nucl. Phys. **B637**, 3 (2002).
[22] J. Breitweg *et al.* (Zeus Collaboration), Nucl. Phys. **B596**, 3 (2001).
[23] A. Aktas *et al.* (H1 Collaboration), Eur. Phys. J. C **41**, 273 (2005).
[24] P. Amaudraz *et al.*, Phys. Rev. Lett. **66**, 2712 (1991); M. Arneodo *et al.*, Phys. Rev. D **50**, R1 (1994); M. Arneodo *et al.*, Phys. Lett. B **364**, 107 (1995).
[25] E. A. Hawker *et al.* (E866/NuSea Collaboration), Phys. Rev. Lett. **80**, 3715 (1998); J. C. Peng *et al.*, Phys. Rev. D **58**, 092004 (1998).
[26] S. Kumano, Phys. Rep. **303**, 183 (1998).
[27] G. T. Garvey and J. C. Peng, Prog. Part. Nucl. Phys. **47**, 203 (2001).
[28] W. Melnitchouk, J. Speth, and A. W. Thomas, Phys. Rev. D **59**, 014033 (1999).
[29] H. Holtmann, A. Szczurek, and J. Speth, Nucl. Phys. **A596**, 631 (1996).
[30] C. Boros and A. W. Thomas, Phys. Rev. D **60**, 074017 (1999).
[31] R. J. Fries and A. Schäfer, Phys. Lett. B **443**, 40 (1998).
[32] F. G. Cao and A. I. Signal, Eur. Phys. J. C **21**, 105 (2001).
[33] S. Kumano and M. Miyama, Phys. Rev. D **65**, 034012 (2002).
[34] F. G. Cao and A. I. Signal, Phys. Rev. D **68**, 074002 (2003).
[35] A. Airapetian *et al.* (HERMES Collaboration), Phys. Rev.

Lett. **92**, 012005 (2004).
[36] R. G. Roberts, *The Structure of the Proton* (Cambridge University Press, Cambridge, 1990).
[37] J. D. Sullivan, Phys. Rev. D **5**, 1732 (1972).
[38] A. W. Thomas, Phys. Lett. **126B**, 97 (1983).
[39] R. L. Jaffe and A. Manohar, Nucl. Phys. **B321**, 343 (1989).
[40] Y. Frishman and E. Gotsman, Phys. Rev. **140**, B1151 (1965).
[41] K. G. Boreskov and A. B. Kaidalov, Eur. Phys. J. C **10**, 143 (1999).
[42] R. J. Fries, A. Schäfer, and C. Weiss, Eur. Phys. J. A **17**, 509 (2003).
[43] F. G. Cao and A. I. Signal, Phys. Lett. B **559**, 229 (2003).
[44] A. Schreiber and A. W. Thomas, Phys. Lett. B **215**, 141 (1988).
[45] S. D. Drell, D. J. Levy, and T.-M. Yan, Phys. Rev. D **1**, 1035 (1970).
[46] S. Weinberg, Phys. Rev. **150**, 1313 (1966).
[47] A. W. Thomas and W. Melnitchouk, in *New Frontiers in Nuclear Physics*, edited by S. Homma, Y. Akaishi, and M. Wada (World Scientific, Singapore, 1994).
[48] J. Speth and A. W. Thomas, Adv. Nucl. Phys. **24**, 83 (1997).
[49] J. B. Kogut and D. E. Soper, Phys. Rev. D **1**, 2901 (1970).
[50] G. P. Lepage and S. J. Brodsky, Phys. Rev. D **22**, 2157 (1980).
[51] R. Machleidt, K. Holinde, and Ch. Elster, Phys. Rep. **149**, 1 (1987).
[52] V. R. Zoller, Z. Phys. C **53**, 443 (1992).
[53] T. DeGrand, R. L. Jaffe, K. Johnson, and J. Kiskis, Phys. Rev. D **12**, 2060 (1975).
[54] A. W. Thomas, Adv. Nucl. Phys. **13**, 1 (1984).
[55] A. I. Signal and A. W. Thomas, Phys. Lett. B **211**, 481 (1988); Phys. Rev. D **40**, 2832 (1989); A. W. Schreiber, A. W. Thomas, and J. T. Londergan, Phys. Rev. D **42**, 2226 (1990).
[56] A. I. Signal, Nucl. Phys. **B497**, 415 (1997).
[57] M. Hirai, S. Kumano, and M. Miyama, Comput. Phys. Commun. **108**, 38 (1998).
[58] L. P. Hoyt and A. I. Signal, in *Proceedings of Lepton Scattering 2001*, edited by W. Melnitchouk, A. Schreiber, and A. W. Thomas (World Scientific, Singapore, 2001), p. 146; A. I. Signal, Int. J. Mod. Phys. A **18**, 1391 (2003).
[59] G. Altarelli and G. G. Ross, Phys. Lett. B **212**, 391 (1988); A. V. Efremov and O. Teryaev, JINR Report No. E2-88-287, 1988.
[60] M. Glück, E. Reya, M. Stratmann, and W. Vogelsang, Phys. Rev. D **63**, 094005 (2001); M. Hirai, S. Kumano, and N. Saito, Phys. Rev. D **69**, 054021 (2004).
[61] S. D. Bass, Acta Phys. Pol. B **34**, 5893 (2003); Rev. Mod. Phys. **77**, 1257 (2005).
[62] S. Wandzura and F. Wilczek, Phys. Lett. **72B**, 195 (1977).
[63] F. M. Steffens, H. Holtmann, and A. W. Thomas, Phys. Lett. B **358**, 139 (1995).
[64] S. A. Larin, T. van Ritbergen, and J. A. M. Vermaseren, Phys. Lett. B **404**, 153 (1997).
[65] While this calculation included incorrect interference terms in the calculations of $\Delta\bar{u}(x)$ and $\Delta\bar{d}(x)$, these terms only contributed to the spin dependent sea at the 10% level.
[66] M. Glück and E. Reya, Mod. Phys. Lett. A **15**, 883 (2000).
[67] X. Ji, Nucl. Phys. **B402**, 217 (1993).